Clonal succession after prolonged antiretroviral therapy rejuvenates CD8+ T cell responses against HIV-1

Eoghann White, Laura Papagno, Assia Samri, Kenji Sugata, Boris P. Hejblum, Amy R Henry, Daniel C Rogan, Samuel Darko, Patricia Recordon-Pinson, Yasmine Dudoit, et al.

Clonal succession after prolonged antiretroviral therapy rejuvenates CD8$^+$ T cell responses against HIV-1

Eoghann WHITE[1,2], Laura PAPAGNO[1], Assia SAMRI[2], Kenji SUGATA[3], Boris HEJBLUM[4], Amy R. HENRY[5], Daniel C. ROGAN[6], Samuel DARKO[5], Patricia RECORDON-PINSON[7], Yasmine DUDOIT[8], Sian LLEWELLYN-LACEY[9], Lisa CHAKRABARTI[10], Florence BUSEYNE[11], Stephen A. MIGUELES[6], David A. PRICE[9,12], Marie-Aline ANDREOLA[7], Yorifumi SATOU[3], Rodolphe THIEBAUT[4,13], Christine KATLAMA[8], Brigitte AUTRAN[2], Daniel C. DOUEK[5] and Victor APPAY[1*]

Running title: CD8$^+$ T cell immunity decades after infection with HIV-1

[1] Université de Bordeaux, CNRS, INSERM, ImmunoConcEpT, UMR 5164, Bordeaux, France
[2] Sorbonne Université, INSERM U1135, Centre d'Immunologie et des Maladies Infectieuses (CIMI-Paris), Paris, France
[3] Division of Genomics and Transcriptomics, Joint Research Center for Human Retrovirus Infection, Kumamoto University, Kumamoto, Japan
[4] Université de Bordeaux, INSERM, Bordeaux Population Health Research Centre, U1219, Inria SISTM, Bordeaux, France
[5] Human Immunology Section, Vaccine Research Center, National Institute of Allergy and Infectious Diseases, National Institutes of Health, Bethesda, Maryland, USA
[6] Laboratory of Immunoregulation, National Institute of Allergy and Infectious Diseases, National Institutes of Health, Bethesda, Maryland, USA
[7] Université de Bordeaux, CNRS, Microbiologie Fondamentale et Pathogénicité, UMR 5234, Bordeaux, France
[8] Sorbonne Université, INSERM, Institut Pierre Louis d'Epidémiologie et de Sante Publique, AP-HP, Pitié Salpêtrière Hospital, Department of Infectious Diseases, Paris, France
[9] Division of Infection and Immunity, Cardiff University School of Medicine, Cardiff, UK
[10] CIVIC Group, Virus and Immunity Unit, Institut Pasteur, Université Paris Cité, CNRS UMR 3569, Paris, France
[11] Unité d'Epidémiologie et Physiopathologie des Virus Oncogènes, Institut Pasteur, Université Paris Cité, CNRS UMR 3569, Paris, France
[12] Systems Immunity Research Institute, Cardiff University School of Medicine, Cardiff, UK
[13] CHU de Bordeaux, Service d'Information Médicale, Bordeaux, France

[*] Correspondence to Victor Appay (victor.appay@immuconcept.org)

ABSTRACT

HIV-1 infection is characterized by a dynamic and persistent state of viral replication that overwhelms the host immune system in the absence of antiretroviral therapy (ART). The impact of prolonged treatment on the antiviral efficacy of HIV-1-specific $CD8^+$ T cells has nonetheless remained unknown. We used single-cell technologies to address this issue in a unique cohort of ageing individuals infected early during the pandemic and subsequently treated with continuous ART. Counterintuitively, we found that long-term treatment was associated with a process of clonal succession, which effectively rejuvenated HIV-1-specific $CD8^+$ T cell populations in the face of immune senescence. Tracking individual transcriptomes further revealed that antecedent clonotypes displayed signatures of exhaustion and terminal differentiation, whereas newly dominant clonotypes displayed signatures of early differentiation and stemness associated with natural control of viral replication. These findings reveal a phenomenal degree of immune resilience that could inform adjunctive treatments for HIV-1.

ONE SENTENCE SUMMARY

Newly dominant clonotypes rejuvenate HIV-1-specific $CD8^+$ T cell immunity after long-term ART.

KEYWORDS

Ageing, ART, $CD8^+$ T cells, HIV-1, TCR.

INTRODUCTION

HIV-1 remains a serious public health challenge for which there is no existing cure or vaccine. A definitive cure would entail complete eradication of the virus throughout the body. This ambitious goal is hampered by the biological nature of HIV-1, which quickly establishes a reservoir of latently infected cells that harbor replication-competent proviruses and persist indefinitely [1, 2]. It may therefore be more realistic to reduce the size of the reservoir below a certain threshold that might allow treatment-free remission without viral recrudescence, a scenario known as functional cure. Most current approaches to functional cure are based on a "shock and kill" strategy, which involves the use of experimental agents to reverse latency and reactivate the reservoir under the cover of antiretroviral therapy (ART), consequently rendering residually infected cells susceptible to immune destruction without further dissemination of HIV-1 [3]. The qualitative properties of antiviral $CD8^+$ T cells will likely be critical for the success of the "kill" component of this strategy, given precedent work in the context of natural immune control of HIV-1 [4].

Effective suppression of viral replication is limited to a rare group of individuals (controllers) in the absence of ART [5]. This phenomenon has been linked with the antiviral efficacy of HIV-1-specific $CD8^+$ T cells that deploy multiple effector functions and proliferate vigrously in response to antigen stimulation [6, 7, 8, 9, 10, 11]. Similar attributes characterize $CD8^+$ T cells specific for HIV-2, which is less pathogenic and more easily controlled than HIV-1 [12, 13, 14]. In contrast, most people living with HIV-1 (PLWH) experience relentless viral replication in the absence of ART, which culminates in the development of AIDS. In these individuals (progressors), ongoing antigen stimulation continually activates and eventually exhausts HIV-1-specific $CD8^+$ T cells, which are subsequently less able to control viral replication [15, 16, 17]. Under these circumstances, HIV-1-specific $CD8^+$ T cells also differentiate progressively, losing expression of CD28 and gaining expression of CD57 [18], a phenotype associated with telomere length erosion and reduced telomerase activity, which are characteristic of senescence [19, 20].

ART can reverse some of the cellular alterations typically observed in progressors by minimizing antigen drive and promoting immune reconstitution [21]. These effects can even extend to the entire $CD8^+$ T cell population, normalizing changes related to activation and differentiation [22, 23]. The extent to which the functionality of HIV-1-specific $CD8^+$ T cells can be restored is nonetheless dependent on the timing of ART. If initiated during chronic infection, ART has a relatively limited ability to correct HIV-1-specific $CD8^+$ T cell dysfunction [24, 25, 26],

but if initiated during primary infection, ART can preserve stem-like HIV-1-specific $CD8^+$ T cells that display functional properties akin to those observed in controllers and individuals infected with HIV-2 [27, 28]. Accordingly, current evidence suggests that ART should be administered at the point of diagnosis to limit immune damage, much of which occurs early after infection with HIV-1.

The gradual loss of immune competence with age, known as immunosenescence, can further undermine the quality of HIV-1-specific $CD8^+$ T cell responses in PLWH. In this context, the most likely scenario to unfold is that HIV-1-specific $CD8^+$ T cells become progressively more dysfunctional over time, especially if ART was initiated during chronic infection, thereby limiting the chances of functional remission in older PLWH. Access to appropriate biological material and technical constraints related to the waning frequencies of HIV-1-specific $CD8^+$ T cells that accompany therapeutically limited viral antigen production have nonetheless thwarted attempts to confirm or refute this possibility. In this study, we used polychromatic flow cytometry and single-cell RNA sequencing (scRNAseq) to characterize the phenotypic and transcriptomic attributes of increasingly rare HIV-1-specific $CD8^+$ T cells isolated from PLWH over a median period of 25 years from diagnosis in the early years of the pandemic, before the widespread introduction of ART. Unexpectedly, we found that long-term therapeutic suppression of viral replication in these individuals was associated with a rejuvenation effect among HIV-1-specific $CD8^+$ T cell populations attributable to the emergence of newly dominant clonotypes, defined by the expression of unique T cell receptors (TCRs).

RESULTS

Ageing and long-term treatment of PLWH

To evaluate the durability of antiviral $CD8^+$ T cell immunity against HIV-1, we accessed a unique biorepository established as part of an initiative termed IMMUNOCO [29, 30, 31]. This cohort study recruited 152 untreated HIV-1-infected adults between 1991 and 1992. Among these participants, 28 underwent regular monitoring until 2016/2017, representing a median duration of 25 years, and 20 donated blood samples at the beginning (EARLY) and end of this time frame (LATE) (**Supplementary Table 1**). In some cases (n = 2), samples were available from the late 1980s, and in other cases (n = 15), samples were available from intermediate (INT) time points in the mid-1990s. All samples were cryopreserved as peripheral blood mononuclear cells (PBMCs).

Participants were untreated at the EARLY time point, treated ineffectively with nucleoside analogue monotherapy at the INT time point, and treated effectively with combination ART for 15 years before the LATE time point (**Fig. 1a**). After the initiation of ART, several individuals continued to experience recurrent episodes of detectable viral replication, which gradually subsided by 2007 (**Fig. 1b** and **Extended Data Fig. 1**). There was a median of 11.6 years between the last major episode of viral replication, defined as >1,000 plasma copies/ml, and the LATE time point. $CD4^+$ T cell counts and CD4/CD8 ratios were significantly higher at the LATE time point compared with the EARLY or INT time points (**Fig. 1c**), consistent with the known benefits of long-term ART.

Inevitably, all participants continued to age throughout the study (**Fig. 1d**). In line with the process of immune senescence [20], the absolute counts and relative frequencies of naive $CD8^+$ T cells in these individuals had declined by the LATE time point, approximating levels observed among older HIV-1-seronegative (age, >75 years) and HIV-1-seropositive individuals (age, >65 years) (**Fig. 1e**). Moreover, these residual naive $CD8^+$ T cell populations harbored shorter telomeres relative to naive $CD8^+$ T cell populations from younger uninfected adults (age, 25–40 years) [32], with lengths approaching those of memory $CD8^+$ T cells expressing the senescence marker CD57 (**Fig. 1f**). Ageing was also associated with the progressive accumulation of highly differentiated memory $CD8^+$ T cells, defined by the loss of CD28 and/or the gain of CD57 (**Fig. 1g**).

HIV-1-specific CD8$^+$ T cells are less differentiated after long-term treatment of PLWH

To extend these findings, we used human leukocyte antigen (HLA) class I-matched tetrameric antigen complexes (tetramers, $n = 13$) to enumerate and track HIV-1-specific CD8$^+$ T cells over time (**Fig. 1a** and **Fig. 2a**), which was enabled by compatible genetic backgrounds in 11 of the 20 participants who had donated samples across the duration of the study (**Supplementary Table 1**). In line with previous reports [24, 33], we detected lower frequencies of tetramer$^+$ CD8$^+$ T cells at the LATE time point compared with the EARLY time point (**Fig. 2b**).

We then assessed the expression of markers associated with cellular differentiation (CD27, CD28, and CD45RA), activation (CD38 and HLA-DR), and replicative senescence (CD57) (**Fig. 2c** and **Extended Data Fig. 2a**). As expected, tetramer$^+$ CD8$^+$ T cells less commonly expressed CD38 at the LATE time point compared with the EARLY or INT time points (**Fig. 2d**), consistent with the long-term suppression of viral replication by ART. However, these cells also less commonly expressed CD57 (**Fig. 2e**) and more commonly expressed the costimulatory receptor CD28 at the LATE time point compared with the EARLY and/or INT time points (**Fig. 2f**), indicating a counterintuitive rejuvenation effect after many years of infection with HIV-1. This phenotype is reminiscent of HIV-2-specific CD8$^+$ T cells, which typically display robust antiviral properties and maintain characteristics of early memory [12, 13, 14], suggesting that HIV-1-specific CD8$^+$ T cells might regain similar attributes under conditions of viral suppression, including the ability to proliferate vigorously and self-renew, despite clear ageing of the immune system. Direct functional verification was nonetheless precluded by the rarity of HIV-1-specific CD8$^+$ T cells at the LATE time point (ranging from 50 to 300 tetramer$^+$ events per 10×10^6 cryopreserved PBMCs).

HIV-1-specific CD8$^+$ T cells are rejuvenated after long-term treatment of PLWH

To circumvent this technical limitation, we harnessed the power of single-cell transcriptomics to characterize HIV-1-specific CD8$^+$ T cells from donors PS03, PS14, PS24, and PS212, all of whom had detectable tetramer$^+$ populations at both the EARLY and LATE time points for comparison. HIV-1-specific CD8$^+$ T cells (n = 100 tetramer$^+$ events) spanning five viral specificities (SL9/HLA-A*02:01, QK10/HLA-A*03:01, EI8/HLA-B*08:01, FL8/HLA-B*08:01, and KF11/HLA-B*57:01) at both time points were index-sorted and processed for scRNAseq. Rare events were accommodated using the SMARTseq approach to capture whole transcriptomes reproducibly. The datasets from PS14 and PS212 did not pass rigorous quality control checks and were excluded in totality. Complete transcriptomic analysis was therefore

limited to the two remaining individuals, namely PS03 (age, 55 years at the LATE time point) and PS24 (age, 78 years at the LATE time point).

Two distinct HIV-1-specific $CD8^+$ T cell populations were analyzed from donor PS24, one targeting the Gag-derived EI8 epitope, and the other targeting the Nef-derived FL8 epitope (**Fig. 3a**). Uniform Manifold Approximation and Projection (UMAP) representation of the data partitioned the transcriptomes into two groups corresponding to the EARLY and LATE time points, irrespective of specificity (**Fig. 3b**). Datasets were therefore merged across specificities to analyze differential gene expression as a function of time (**Fig. 3c**, **d**). Among the top 142 genes enriched at the EARLY time point were *Ly6e*, *Cemip2*, *Ifi44l*, *Ifi6*, *Riok3*, and *Ifitm1*, suggestive of a type I interferon (IFN) signature. EARLY cells were characterized by an overall effector-like profile (*e.g.*, *Gzmb*, *Gzmh*, *Fgfbp2*, and *Ccl4* – not shown) and exhibited relative overexpression of genes associated with inhibitory pathways (*e.g.*, *Prdm1* and *Adgrg1*) and exhaustion (*e.g.*, *Tox*) (**Fig. 3e**). In contrast, LATE cells exhibited relative overexpression of genes associated with self-renewal (*e.g.*, *Il7r* and *Cxcr4*) and stemness (*e.g.*, *Gzmk*, *Ccr7*, *Sell*, *Bcl6*, and *Klf2*) (**Fig. 3e**). A similar picture emerged from analyses of HIV-1-specific $CD8^+$ T cell populations targeting the Gag-derived KF11 epitope in donor PS03. In particular, EARLY cells were characterized by an IFN-like signature (*e.g.*, *Ifi27*, *Ifi44l*, *Ifi6*, and *Isg15*) and relative overexpression of genes associated with inhibitory pathways (*e.g.*, *Prdm1* and *Havcr2*), whereas LATE cells preferentially expressed genes associated with self-renewal (*e.g.*, *Tcf7*, *Il7r*, and *Nell2*) and stemness (*e.g.*, *Gzmk*) (**Extended Data Fig. 3a**–**3e**). Moreover, expression of the stemness marker TCF-1, encoded by *Tcf7*, was largely confined to naive and $CD28^+$ memory $CD8^+$ T cells (**Extended Data Fig. 2b**), and HIV-1-specific $CD8^+$ T cells from untreated progressors less commonly expressed TCF-1 than HIV-1-specific $CD8^+$ T cells from PLWH treated with long-term ART (**Extended Data Fig. 2c**, **2d**), consistent with the findings of a previous study [26].

These observations were confirmed using normalized counts to perform a gene set enrichment analysis (GSEA), which further revealed that EARLY cells preferentially expressed genes associated with apoptosis and programmed cell death (**Fig. 3f** and **Extended Data Fig. 3f**). In addition, EARLY cells displayed a gene signature reminiscent of terminal differentiation, typically associated with the expression of KLRG1. In contrast, LATE cells were enriched for genes associated with early differentiation and protein translation (**Fig. 3g** and **Extended Data Fig. 3f**), which have been linked with natural control of HIV-1 [34].

HIV-1-specific CD8$^+$ T cells exhibit a controller-like profile after long-term treatment of PLWH

To pursue this line of investigation, we mined publicly available datasets reporting the transcriptomes of HIV-1-specific CD8$^+$ T cells isolated from individuals defined as natural controllers or progressors in the absence of ART [35]. As expected, EARLY cells resembled HIV-1-specific CD8$^+$ T cells from progressors transcriptomically, with gene expression profiles indicative of IFN signaling (*e.g.*, *Ifi44l*) and negative regulation (*e.g.*, *Adgrg1*) (**Fig. 4a**). In contrast, LATE cells were more akin to HIV-1-specific CD8$^+$ T cells from controllers transcriptomically, with gene expression profiles characteristic of stemness (*e.g.*, *Ccr7*, *Cxcr3*, and *Nell2*) and upregulation of the protein translation machinery (*e.g.*, *Rps16*) (**Fig. 4b**).

To validate this comparison, we index-sorted CD8$^+$ T cells targeting the HLA-B*53:01-restricted Gag-derived epitope TL9 from two donors exhibiting natural control of HIV-2. These cells typically display potent antiviral functionality and commonly express CD28 (**Extended Data Fig. 4a**) [12, 13, 14]. We then analyzed the transcriptomes of these HIV-2-specific CD8$^+$ T cells using scRNAseq. Principal component analysis (PCA) yielded three clusters matching each group in comparisons with the transcriptomes of HIV-1-specific CD8$^+$ T cells, namely EARLY, LATE, and HIV-2. LATE cells clustered in close proximity with HIV-2-specific CD8$^+$ T cells and overlapped with cells expressing CD28 (**Fig. 4c**). Unsupervised analyses of differentially expressed genes (i.e. 532 genes with FDR-corrected *P* values < 0.001) further yielded a clear partition between EARLY and LATE/HIV-2 (**Extended Data Fig. 4b**). These latter cells were linked by relative overexpression of genes associated with early differentiation and stemness (*e.g.*, *Gzmk*, *Tcf7*, *Il7r*, and *Nell2*) and relative underexpression of genes associated with effector functionality and exhaustion (**Fig. 4d**).

To extend these findings, we performed functional assays of cytotoxic activity and proliferative capacity, which are established correlates of CD8$^+$ T cell efficacy against HIV-1 [8, 36]. Cytotoxic activity was assessed indirectly via the expression of granzyme B and perforin [37], and proliferative capacity was assessed directly via numerical expansion in response to peptide stimulation **(Fig. 4e**). Proliferative capacity was significantly impaired among HIV-1-specific CD8$^+$ T cells from untreated progressors versus PLWH treated with long-term ART (**Fig. 4f**, **4g**). The ability to upregulate cytotoxic molecules, especially granzyme B, followed a similar pattern (**Fig. 4h**, **4i**). No such functional differences were detected in similar comparisons of

HIV-1-specific CD8$^+$ T cells from natural controllers versus PLWH treated with long-term ART.

HIV-1-specific CD8$^+$ T cells are replaced after long-term treatment of PLWH

The data presented above could potentially be explained by clonal succession, whereby new clonotypes are recruited to replace old clonotypes with the same antigen specificity, or by a process of dedifferentiation and recovery from exhaustion among HIV-1-specific CD8$^+$ T cells expressing the same TCR. Each of these scenarios could further be influenced by immune adaptation to viral escape, which can almost completely reshape the landscape of antigen sequences in the latent reservoir after the initiation of ART [38]. To address this issue, we first sequenced the targeted viral epitope regions in PBMCs from donors PS03, PS14, PS17, PS24, PS112, and PS114. Unexpectedly, the dominant antigen species were generally maintained between the EARLY and/or INT time points and the LATE time point (**Extended Data Fig. 5**), excluding a primary role for viral evolution in the rejuvenation of HIV-1-specific CD8$^+$ T cells after long-term ART.

We then assessed the clonotypic composition of HIV-1-specific CD8$^+$ T cell populations over time, identifying single-cell TCRα (*TRA*) and TCRβ (*TRB*) gene rearrangements from the scRNAseq data generated for PS03 (KF11/HLA-B*57:01) and PS24 (EI8/HLA-B*08:01 and FL8/HLA-B*08:01). The repertoires of all three HIV-1-specific CD8$^+$ T cell populations changed markedly between the EARLY and/or INT time points and the LATE time point, and new clonotypes were detected at the LATE time point (**Fig. 5a**–**c** and **Extended Data Fig. 6a**–**c**). In donor PS24, an FL8-specific TRBV5-6/TRBJ2-5 clonotype was highly dominant at the EARLY and INT time points but subdominant at the LATE time point, succeeded after 25 years by an FL8-specific TRBV2/TRBJ2-7 clonotype (**Fig. 5a** and **Extended Data Fig. 6a**). Similarly, an EI8-specific TRBV9/TRBJ2-5 clonotype was identified at all time points in donor PS24, but newly detected EI8-specific clonotypes (TRBV9/TRBJ1-2 and TRBV20-1/TRBJ2-7) predominated at the LATE time point (**Fig. 5b** and **Extended Data Fig. 6b**). In donor PS03, a KF11-specific TRBV5-6/TRBJ1-5 clonotype that predominated at the EARLY time point was superseded by another KF11-specific TRBV5-6/TRBJ1-5 clonotype at the LATE time point (**Fig. 5c** and **Extended Data Fig. 6c**).

These findings were confirmed using samples from another donor, VA02, recruited from a geographically distinct site. In this case, we were able to conduct a detailed longitudinal

analysis of $CD8^+$ T cells targeting the HLA-B*27:05-restricted Gag-derived epitope KK10 over a time period of 11 years from the initiation of ART (**Extended Data Fig. 7a**). KK10-specific $CD8^+$ T cells from donor VA02 more commonly expressed CD28 over time (**Extended Data Fig. 7b**) and exhibited progressive changes in gene transcription, acquiring a less exhausted and more stem-like profile by the LATE time point (**Extended Data Fig. 7c**, **7d**). Moreover, these changes were associated with a shift in clonal dominance, as observed in donors PS03 and PS24. Specifically, the initially dominant TRBV5-4/TRBJ2-7, TRBV7-9/TRBJ2-3, and TRBV4-3/TRBJ2-7 clonotypes were progressively superseded by a TRBV7-9/TRBJ2-7 clonotype, which was subdominant before the initiation of ART (**Extended Data Fig. 7e**).

On the basis of these data, we were able to define the gene expression profiles of old and newly dominant clonotypes at the LATE time point, although low cell numbers limited this analysis to the FL8-specific population from donor PS24 and the KK10-specific population from donor VA02. A sparse Partial Least Squares Discriminant Analysis (sPLS-DA) of FL8-specific $CD8^+$ T cells from donor PS24 highlighted a separation between the two clonotypes associated with 50 variables along component 1 (**Fig. 5d**). Many upregulated genes in the old clonotype were associated with exhaustion and negative regulation, including *Cd160*, which encodes an inhibitory receptor that interacts with TNFRSF14, *Nr3c1*, which encodes a glucocorticoid receptor known to promote tumor-infiltrating lymphocyte dysfunction, and *Mat2a*, which encodes an enzyme involved in methionine metabolism that drives exhaustion via the production of S-adenosylmethionine [39, 40, 41] (**Fig. 5e**). Moreover, GSEA confirmed the enrichment of inhibitory genes and revealed that several pathways characteristic of EARLY cells were still active in the old clonotype at the LATE time point, highlighting signatures associated with apoptosis, IFN signaling, terminal exhaustion, and the p53 pathway (**Fig. 5f**). In contrast, the newly dominant clonotype exhibited gene signatures associated with naive cells and central memory differentiation, indicating an antithetical transcriptomic profile that segregated with the expression of a distinct TCR (**Fig. 5f**). Similarly, the newly dominant KK10-specific clonotype in VA02 exhibited a more pronounced stem-like profile at the LATE time point relative to the previously dominant clonotype, further linking a defined pattern of gene expression with the phenomenon of clonal succession (**Extended Data Fig. 7f**).

The indexed nature of our flow cytometric sorting strategy for scRNAseq further allowed us to track the phenotype of old and newly dominant clonotypes over time. Using this approach, we found that newly dominant clonotypes more frequently expressed CD28, our initial parameter

of differentiation, compared with old clonotypes in donors PS03 and PS24 (**Fig. 5g**). We then conducted a final series of experiments to exclude the possibility that these phenotypic and transcriptomic differences were not simply related to corresponding differences in antigen avidity, which is known to impact antiviral efficacy [7, 10]. For this purpose, we transduced paired TCRα and TCRβ chains from old and newly dominant clonotypes into TCR-deficient Jurkat cells and performed tetramer dilution assays, measuring uptake as a function of concentration via flow cytometry (**Extended Data Fig. 8**). Similar profiles were observed for the old and newly dominant KF11-specific clonotypes from donor PS03, whereas greater avidity was observed for the newly dominant FL8-specific clonotype versus the old FL8-specific clonotype from donor PS24 (**Fig. 5h**).

Collectively, the findings demonstrate that clonal succession, without a concomitant reduction in antigen avidity, can rejuvenate HIV-1-specific $CD8^+$ T cell populations after long-term treatment with ART.

DISCUSSION

In this study, we tracked the evolution of HIV-1-specific $CD8^+$ T cells over a median time period of 25 years, enabled by access to a unique biorepository of samples collected from PLWH. Although rare, HIV-1-specific $CD8^+$ T cells were still detectable at the end point of observation, despite effective long-term treatment of all participants with ART. Unexpectedly, these cells displayed characteristics associated with early differentiation, including surface expression of CD28 [42], and stemness, exemplified by the upregulation of *Tcf7*, which encodes TCF-1. CD28 is a costimulatory receptor that facilitates antigen-driven activation, proliferation, and survival among cognate T cell populations [43], where loss of expression acts as a marker of senescence [44, 45], and TCF-1 is a critical regulator of memory differentiation and persistence [46]. TCF-1 is considered essential for the maintenance of $CD8^+$ T cell efficacy [47]. It is notable here that virus-specific $CD8^+$ T cells expressing TCF-1 have been associated with natural control of HIV-1 and SIV [26, 48, 49]. The functional preservation of HIV-1-specific $CD8^+$ T cells in patients who initiated ART during primary infection has also been linked with a stem-like phenotype, defined by the expression of TCF-1 [28].

TCR repertoire analyses revealed that old clonotypes present at the EARLY and/or INT time points were generally replaced by newly dominant clonotypes at the LATE time point, indicating clonal succession. This phenomenon was not associated with viral escape. Our experimental approach further allowed us to characterize the gene expression profiles of individual clonotypes at the LATE time point, generating unique insights into the coincident process of apparent rejuvenation. Of particular note, we found that newly dominant clonotypes overexpressed genes associated with early differentiation and a stem-like profile, whereas old clonotypes overexpressed genes associated with apoptosis, exhaustion, IFN signaling, negative regulation, and terminal differentiation. Index tracking confirmed the observation that newly dominant clonotypes preferentially expressed the early differentiation marker CD28. Moreover, these phenotypic and transcriptomic differences were not obviously related to differences in antigen avidity, which can regulate cell fate as a function of signals transduced via the TCR. It therefore seems likely that ongoing viral replication below the limit of detection, especially in the context of full immune reconstitution, resulted in the *de novo* priming of new clonotypes and/or the expansion of early memory clonotypes exhibiting optimal functional properties associated with natural control of HIV-1. These observations are consistent with recent work demonstrating that HIV-1-specific $CD8^+$ T cell frequencies correlate directly with measures of

cell-associated HIV-1 DNA and RNA during continuous ART [50, 51] and could also help explain the link between antiviral efficacy and the expression of distinct TCRs [52].

Our investigations were constrained by sample size, reflecting the inherent challenges associated with longitudinal human studies in terms of recruitment, retention, and the collection and storage of biological material over extended periods of time. Functional studies were also hindered by the very low frequencies of HIV-1-specific $CD8^+$ T cells detected after prolonged therapeutic suppression of viral replication in PLWH. Our phenotypic and transcriptomic data nonetheless provide a first glimpse into a process of clonal succession that rejuvenates HIV-1-specific $CD8^+$ T cell populations after long-term ART. It remains unclear to what extent this effect might be associated with genuine antiviral efficacy. However, the existence of such a mechanism could facilitate the development of new interventional approaches to boost antiviral $CD8^+$ T cell immunity, potentially enabling functional cure of HIV-1.

PLWH typically exhibit sustained immune dysfunction reminiscent of senescence, even after treatment with ART [53, 54, 55]. These features, including the accumulation of $CD8^+$ T cells with a $CD28^-/CD57^+$ phenotype, become exacerbated with age, reflecting a progressive loss of naive precursors and hematopoietic progenitors over time [56]. It is particularly remarkable in this context that clonal succession occurred despite a limited capacity for immune reconstitution in our cohort of ageing PLWH. The phenomenon of rejuvenation via this process under such extreme circumstances nonetheless highlights the resilience of the cellular immune system. Accordingly, our findings could have broad implications for the prophylactic or therapeutic induction of *de novo* $CD8^+$ T cell responses in people with various forms of immune compromise, including the elderly and PLWH.

ONLINE METHODS

Donors

HIV-1-infected adults (n = 152) were enrolled in a prospective study between 1991 and 1992. Exclusion criteria were haemophilia and ongoing intravenous drug use. Seropositivity was confirmed via Western blot and ELISA. A subset of these patients (n = 28) underwent continual monitoring every 2–3 months until 2016/2017 (median duration = 25 years). Nucleoside analogue therapy was initiated or maintained according to local clinical practice from November 1991 to March 1996. Combination therapy was used to control viral replication from 2001/2002. Longitudinal samples from another HIV-1-infected adult were obtained from the National Institutes of Health (NIH). In this case, ART was initiated in February 2008, and follow-up occurred until September 2019. Additional samples from untreated progressors, untreated controllers with HIV-1 load below 400 copies/ml for >3 years, and PLWH with effective therapeutic suppression of viral replication for >10 years after the initiation of continuous ART were obtained from the Pitié-Salpétrière Hospital (Paris, France). All donors provided written informed consent in accordance with the principles of the Declaration of Helsinki. The use of blood products from anonymized HIV-1-infected participants was approved by the Comité de Protection des Personnes of the Pitié-Salpétrière Hospital (Paris, France) or the National Institute of Allergy and Infectious Diseases (NIAID) Institutional Review Board (NIH, USA).

Flow cytometry

HIV-1-specific $CD8^+$ T cells were identified using the following HLA class I tetramers conjugated to PE: SLYNTVATL (SL9/HLA-A*02:01), QVPLRPMTYK (QK10/HLA-A*03:01), RLRPGGKKKY (RY10/HLA-A*03:01), EIYKRWII (EI8/HLA-B*08:01), FLKEKGGL (FL8/HLA-B*08:01), KRWIILGLNK (KK10/HLA-B*27:05), KAFSPEVIPMF (KF11/HLA-B*57:01), and TSTLQEQIGW (TW10/HLA-B*57:01). PBMCs were labeled with LIVE/DEAD Fixable Aqua (Thermo Fisher Scientific) for 10 min at room temperature and then stained consecutively with tetramer–PE for 15 min at 37 °C and the following directly conjugated monoclonal antibodies for 15 min at room temperature: anti-CD4–BV650 (clone SK3, BD Biosciences), anti-CD8–APC-Cy7 (clone SK1, BD Biosciences), anti-CD27–AF700 (clone O323, BioLegend), anti-CD28–PE-CF594 (clone CD28.2, BD Biosciences), anti-CD38–APC (clone HB7, BD Biosciences), anti-CD45RA–V450 (clone HI100, BD Biosciences), anti-CD57–BV605 (clone NK-1, BD Biosciences), anti-CD95–FITC (clone

DX2, BD Biosciences), and anti-HLA-DR–PerCP-Cy5.5 (clone L243, BD Biosciences). Stained cells were fixed in 1% paraformaldehyde (Thermo Fisher Scientific). In some experiments, cells were fixed/permeabilized using a Transcription Factor Buffer Set (BD Biosciences), stained intracellularly with anti-TCF-1–AF647 (clone S33-966, BD Biosciences) for 40 min at 4 °C, and washed in Perm/Wash Buffer (BD Biosciences). Data were acquired using an LSRFortessa (BD Biosciences) and analyzed using FlowJo software version 10.8 (FlowJo LLC). The gating strategy is shown in **Extended Data Fig. 9.**

Telomere length measurement

Telomere lengths were measured as described previously [32]. Briefly, genomic DNA was extracted from flow-sorted cells using a QIAmp DNA Mini Kit (QIAGEN) and quantified using a NanoDrop 2000 (Thermo Fisher Scientific). Relative telomere length was measured as the ratio of standard DNA quantities for telomere template (T) over single-copy gene 36B4 (S) determined via qRT-PCR from 2 ng of genomic DNA. Actual telomere length was derived from simultaneous analyses of serially diluted DNA extracted from 293T cells and run in parallel using Southern blotting and qRT-PCR.

scRNAseq

HIV-1-specific $CD8^+$ T cells (n = 100 $tetramer^+$ events) were index-sorted into 96-well microtiter plates containing lysis buffer (Takara Bio) using a BD FACSAria II (BD Biosciences) and frozen immediately at −80 °C. Libraries were prepared using a SMART-Seq v4 Ultra Low Input RNA Kit (Takara Bio). cDNA was amplified and indexed using a Nextera XT DNA Library Preparation Kit (Illumina). Hashtag-labeled KK10-specific $CD8^+$ T cells (n = 4,903–10,000 $tetramer^+$ events) from donor VA02 were bulk-sorted and processed using standard procedures for scRNAseq (10x Genomics). Pooled libraries were quantified and sequenced across 150 bp using a paired-end strategy with a HiSeq 3000 System (Illumina).

Transcriptome analysis

Fastq files were aligned to the hg38 genome build using STAR software version 2.7.0. Aligned files were pooled and imported in R. Quality control was performed using scater version 3.19 with the following metrics: library size, number of expressed features, and proportion of reads mapped to the mitochondrial genome [57]. Outlier cells were identified for each metric based on the median absolute deviation (MAD) from the median value of each metric across all cells, with the cutoff for exclusion set at >3 MADs. Fixed thresholds were also used to exclude cells

expressing <500 or >5,000 genes, or expressing more than 5 % of mitochondrial genes. This approach yielded 73, 230, and 123 quality-controlled cells from PS03, PS24, and HIV-2 controllers (n = 2), respectively. Retained cells were normalized using scran version 1.20.1, which implements the deconvolution strategy for scaling normalization [58]. For VA02, cells were excluded when expressing less than 200 genes or more than 2500 genes or when expressing more than 5 % of mitochondrial genes, retaining a total of 18.268 cells after quality control (between 2095 and 3967 cells at each time point). Gene expression normalization was performed using the NormalizeData() function from Seurat. Differentially expressed genes were detected using the *findMarkers* function (scran), with the FDR-corrected cutoff set at $P <$ 0.05 (Wilcoxon unpaired test). Violin plots were generated using the *VlnPlot* function in Seurat version 4.1.1. Heatmaps and volcano plots were generated using pheatmap version 1.0.12 and ggplot2 version 3.3.6, respectively. GSEA was conducted using software developed by the Broad Institute [59]. sPLS-DA was performed as described previously [60] .

Functional assays

PBMCs were thawed and resuspended at 5×10^6 cells/well in 48-well culture plates (Thermo Fisher Scientific) containing AIM V medium (Thermo Fisher Scientific) supplemented with 50 ng/ml FMS-like tyrosine kinase 3 ligand (FLT3L, R&D Systems). After 24 h (day 1), cells were stimulated with the relevant cognate peptide at a final concentration of 0.1 μM. On day 2, fetal bovine serum was added at a final v/v ratio of 10%. Medium was replaced every 3 days thereafter with fresh RPMI 1640 (Thermo Fisher Scientific) supplemented with 10% fetal bovine serum (Thermo Fisher Scientific) and 1% penicillin/streptomycin (Thermo Fisher Scientific). On day 0 and day 12, cells were labeled with LIVE/DEAD Fixable Aqua (Thermo Fisher Scientific) for 10 min at room temperature, stained consecutively with tetramer–PE for 15 min at 37 °C and anti-CD8–APC-Cy7 (clone SK1, BD Biosciences) for 15 min at room temperature, fixed/permeabilized using a Transcription Factor Buffer Set (BD Biosciences), stained intracellularly with anti-granzyme B–V450 (clone GB11, BD Biosciences) and anti-perforin–FITC (clone B-D48, BioLegend) for 40 min at 4 °C, and washed in Perm/Wash Buffer (BD Biosciences). Data were acquired using an LSRFortessa (BD Biosciences) and analyzed using FlowJo software version 10.8 (FlowJo LLC).

Clonotype analysis

Fastq files were processed for *TRA* and *TRB* annotation using MiXCR version 3.0.13 (https://mixcr.com). Sequence data were analyzed using immunarch version 0.7.0 in R.

PCR amplification and sequencing of Gag and Nef

Viral DNA was extracted from PBMCs. Gag and Nef were amplified from extracted DNA using previously reported primers [61] and ThermoStar 2 Hot Start Taq (Eurobio). PCR products were sequenced across both strands using an Applied Biosystems 3500xL Dx Genetic Analyzer with primers from the second PCR.

TCR avidity measurements

FL8-specific and KF11-specific TCRs from old and newly dominant clonotypes identified via scRNAseq were reconstituted in TCR-deficient Jurkat cells [62], alongside CD8α and CD8β [63]. CD8/TCR-transduced Jurkat cells were magnetically enriched using anti-CD3–FITC (clone SK7, BioLegend) in conjunction with Anti-FITC MicroBeads (Miltenyi Biotec). TCR avidity was measured using tetramer dilution assays. Briefly, CD8/TCR-transduced Jurkat cells were incubated with serial 1/3 dilutions of cognate tetramer spanning concentrations from 200 μg/ml to 0.0008 μg/ml for 30 min at room temperature, and tetramer$^+$ cells were quantified via flow cytometry. TCR-expressing Jurkat E6.1 cells were used as a control for nonspecific tetramer uptake.

General statistics

Group comparisons were performed using a two-tailed Mann–Whitney U test. Correlations were assessed using Spearman's rank test. All statistical analyses were performed using untransformed data in Prism version 9 (GraphPad) and/or R. Significance was assigned at $P < 0.05$.

Data availability

All data reported in this paper will be shared by the corresponding author upon reasonable request.

REFERENCES

1. Finzi, D. *et al.* Identification of a reservoir for HIV-1 in patients on highly active antiretroviral therapy. *Science* **278**, 1295–1300 (1997).

2. Wong, J.K. *et al.* Recovery of replication-competent HIV despite prolonged suppression of plasma viremia. *Science* **278**, 1291–1295 (1997).

3. Hamer, D.H. Can HIV be cured? Mechanisms of HIV persistence and strategies to combat it. *Curr HIV Res* **2**, 99–111 (2004).

4. Appay, V., Douek, D.C. & Price, D.A. $CD8^+$ T cell efficacy in vaccination and disease. *Nat Med* **14**, 623–628 (2008).

5. Saez-Cirion, A., Pancino, G., Sinet, M., Venet, A. & Lambotte, O. HIV controllers: how do they tame the virus? *Trends Immunol* **28**, 532–540 (2007).

6. Betts, M.R. *et al.* HIV nonprogressors preferentially maintain highly functional HIV-specific $CD8^+$ T cells. *Blood* **107**, 4781–4789 (2006).

7. Almeida, J.R. *et al.* Superior control of HIV-1 replication by $CD8^+$ T cells is reflected by their avidity, polyfunctionality, and clonal turnover. *J Exp Med* **204**, 2473–2485 (2007).

8. Migueles, S.A. *et al.* Lytic granule loading of $CD8^+$ T cells is required for HIV-infected cell elimination associated with immune control. *Immunity* **29**, 1009–1021 (2008).

9. Saez-Cirion, A. *et al.* HIV controllers exhibit potent CD8 T cell capacity to suppress HIV infection ex vivo and peculiar cytotoxic T lymphocyte activation phenotype. *Proc Natl Acad Sci U S A* **104**, 6776–6781 (2007).

10. Almeida, J.R. *et al.* Antigen sensitivity is a major determinant of $CD8^+$ T-cell polyfunctionality and HIV-suppressive activity. *Blood* **113**, 6351–6360 (2009).

11. Hersperger, A.R. *et al.* Perforin expression directly ex vivo by HIV-specific CD8 T-cells is a correlate of HIV elite control. *PLoS Pathog* **6**, e1000917 (2010).

12. Duvall, M.G. *et al.* Polyfunctional T cell responses are a hallmark of HIV-2 infection. *Eur J Immunol* **38**, 350–363 (2008).

13. Leligdowicz, A. *et al.* Highly avid, oligoclonal, early-differentiated antigen-specific $CD8^+$ T cells in chronic HIV-2 infection. *Eur J Immunol* **40**, 1963–1972 (2010).

14. Angin, M. *et al.* Preservation of lymphopoietic potential and virus suppressive capacity by $CD8^+$ T cells in HIV-2-infected controllers. *J Immunol* **197**, 2787–2795 (2016).

15. Day, C.L. *et al.* PD-1 expression on HIV-specific T cells is associated with T-cell exhaustion and disease progression. *Nature* **443**, 350–354 (2006).

16. Wherry, E.J. T cell exhaustion. *Nat Immunol* **12**, 492–499 (2011).

17. Buggert, M. *et al.* T-bet and Eomes are differentially linked to the exhausted phenotype of $CD8^+$ T cells in HIV infection. *PLoS Pathog* **10**, e1004251 (2014).

18. Papagno, L. *et al.* Immune activation and $CD8^+$ T-cell differentiation towards senescence in HIV-1 infection. *PLoS Biol* **2**, E20 (2004).

19. Lichterfeld, M. *et al.* Telomerase activity of HIV-1-specific $CD8^+$ T cells: constitutive up-regulation in controllers and selective increase by blockade of PD ligand 1 in progressors. *Blood* **112**, 3679–3687 (2008).

20. Appay, V. & Sauce, D. Assessing immune aging in HIV-infected patients. *Virulence* **8**, 529–538 (2017).

21. Jain, V. *et al.* Antiretroviral therapy initiated within 6 months of HIV infection is associated with lower T-cell activation and smaller HIV reservoir size. *J Infect Dis* **208**, 1202–1211 (2013).

22. Behrens, N.E., Wertheimer, A., Klotz, S.A. & Ahmad, N. Reduction in terminally differentiated T cells in virologically controlled HIV-infected aging patients on long-term antiretroviral therapy. *PLoS One* **13**, e0199101 (2018).

23. Perdomo-Celis, F., Taborda, N.A. & Rugeles, M.T. $CD8^+$ T-cell response to HIV infection in the era of antiretroviral therapy. *Front Immunol* **10**, 1896 (2019).

24. Appay, V. *et al.* Persistent HIV-1-specific cellular responses despite prolonged therapeutic viral suppression. *AIDS* **16**, 161–170 (2002).

25. Migueles, S.A. *et al.* Defective human immunodeficiency virus-specific $CD8^+$ T-cell polyfunctionality, proliferation, and cytotoxicity are not restored by antiretroviral therapy. *J Virol* **83**, 11876–11889 (2009).

26. Rutishauser, R.L. *et al.* TCF-1 regulates HIV-specific $CD8^+$ T cell expansion capacity. *JCI Insight* **6**, e136648 (2021).

27. Oxenius, A. *et al.* Early highly active antiretroviral therapy for acute HIV-1 infection preserves immune function of $CD8^+$ and $CD4^+$ T lymphocytes. *Proc Natl Acad Sci U S A* **97**, 3382–3387 (2000).

28. Takata, H. *et al.* Long-term antiretroviral therapy initiated in acute HIV infection prevents residual dysfunction of HIV-specific $CD8^+$ T cells. *EBioMedicine* **84**, 104253 (2022).

29. Chouquet, C. *et al.* Correlation between breadth of memory HIV-specific cytotoxic T cells, viral load and disease progression in HIV infection. *AIDS* **16**, 2399–2407 (2002).

30. Haas, G. *et al.* Cytotoxic T-cell responses to HIV-1 reverse transcriptase, integrase and protease. *AIDS* **12**, 1427–1436 (1998).

31. Kousignian, I. *et al.* Markov modelling of changes in HIV-specific cytotoxic T-lymphocyte responses with time in untreated HIV-1 infected patients. *Stat Med* **22**, 1675–1690 (2003).

32. Fali, T. *et al.* New insights into lymphocyte differentiation and aging from telomere length and telomerase activity measurements. *J Immunol* **202**, 1962–1969 (2019).

33. Addo, M.M. *et al.* Comprehensive epitope analysis of human immunodeficiency virus type 1 (HIV-1)-specific T-cell responses directed against the entire expressed HIV-1 genome demonstrate broadly directed responses, but no correlation to viral load. *J Virol* **77**, 2081–2092 (2003).

34. Buggert, M. *et al.* Identification and characterization of HIV-specific resident memory $CD8^+$ T cells in human lymphoid tissue. *Sci Immunol* **3**, eaar4526 (2018).

35. Quigley, M. *et al.* Transcriptional analysis of HIV-specific $CD8^+$ T cells shows that PD-1 inhibits T cell function by upregulating BATF. *Nat Med* **16**, 1147–1151 (2010).

36. Migueles, S.A. *et al.* HIV-specific $CD8^+$ T cell proliferation is coupled to perforin expression and is maintained in nonprogressors. *Nat Immunol* **3**, 1061–1068 (2002).

37. Migueles, S.A. *et al.* Antigenic restimulation of virus-specific memory $CD8^+$ T cells requires days of lytic protein accumulation for maximal cytotoxic capacity. *J Virol* **94**, e10595-20 (2020).

38. Deng, K. *et al.* Broad CTL response is required to clear latent HIV-1 due to dominance of escape mutations. *Nature* **517**, 381–385 (2015).

39. Bozorgmehr, N. *et al.* Expanded antigen-experienced $CD160^+CD8^+$ effector T cells exhibit impaired effector functions in chronic lymphocytic leukemia. *J Immunother Cancer* **9**, e002189 (2021).

40. Acharya, N. *et al.* Endogenous glucocorticoid signaling regulates $CD8^+$ T cell differentiation and development of dysfunction in the tumor microenvironment. *Immunity* **53**, 658–671.e6 (2020).

41. Hung, M.H. *et al.* Tumor methionine metabolism drives T-cell exhaustion in hepatocellular carcinoma. *Nat Commun* **12**, 1455 (2021).

42. Appay, V. *et al.* Memory $CD8^+$ T cells vary in differentiation phenotype in different persistent virus infections. *Nat Med* **8**, 379–385 (2002).

43. Weng, N.P., Akbar, A.N. & Goronzy, J. $CD28^-$ T cells: their role in the age-associated decline of immune function. *Trends Immunol* **30**, 306–312 (2009).

44. Effros, R.B. *et al.* Shortened telomeres in the expanded $CD28^-CD8^+$ cell subset in HIV disease implicate replicative senescence in HIV pathogenesis. *AIDS* **10**, F17–22 (1996).

45. Vallejo, A.N. *et al.* Molecular basis for the loss of CD28 expression in senescent T cells. *J Biol Chem* **277**, 46940–46949 (2002).

46. Zhou, X. *et al.* Differentiation and persistence of memory CD8$^+$ T cells depend on T cell factor 1. *Immunity* **33**, 229–240 (2010).

47. Zehn, D., Thimme, R., Lugli, E., de Almeida, G.P. & Oxenius, A. 'Stem-like' precursors are the fount to sustain persistent CD8$^+$ T cell responses. *Nat Immunol* **23**, 836–847 (2022).

48. Passaes, C. *et al.* Optimal maturation of the SIV-specific CD8$^+$ T cell response after primary infection is associated with natural control of SIV: ANRS SIC Study. *Cell Rep* **32**, 108174 (2020).

49. Angin, M. *et al.* Metabolic plasticity of HIV-specific CD8$^+$ T cells is associated with enhanced antiviral potential and natural control of HIV-1 infection. *Nat Metab* **1**, 704–716 (2019).

50. Takata, H. *et al.* An active HIV reservoir during ART is associated with maintenance of HIV-specific CD8$^+$ T cell magnitude and short-lived differentiation status. *Cell Host Microbe* **31**, 1494–1506.e4 (2023).

51. Dube, M. *et al.* Spontaneous HIV expression during suppressive ART is associated with the magnitude and function of HIV-specific CD4$^+$ and CD8$^+$ T cells. *Cell Host Microbe* **31**, 1507–1522.e5 (2023).

52. Lissina, A., Chakrabarti, L.A., Takiguchi, M. & Appay, V. TCR clonotypes: molecular determinants of T-cell efficacy against HIV. *Curr Opin Virol* **16**, 77–85 (2016).

53. Appay, V. & Kelleher, A.D. Immune activation and immune aging in HIV infection. *Current Opinion HIV AIDS* **11**, 242–249 (2016).

54. Babu, H. *et al.* Systemic inflammation and the increased risk of inflamm-aging and age-associated diseases in people living with HIV on long-term suppressive antiretroviral therapy. *Front Immunol* **10**, 1965 (2019).

55. Lagathu, C. *et al.* Basic science and pathogenesis of ageing with HIV: potential mechanisms and biomarkers. *AIDS* **31 Suppl 2**, S105–S119 (2017).

56. Appay, V. *et al.* Old age and anti-cytomegalovirus immunity are associated with altered T-cell reconstitution in HIV-1-infected patients. *AIDS* **25**, 1813–1822 (2011).

57. McCarthy, D.J., Campbell, K.R., Lun, A.T. & Wills, Q.F. Scater: pre-processing, quality control, normalization and visualization of single-cell RNA-seq data in R. *Bioinformatics* **33**, 1179–1186 (2017).

58. Lun, A.T., Bach, K. & Marioni, J.C. Pooling across cells to normalize single-cell RNA sequencing data with many zero counts. *Genome Biol* **17**, 75 (2016).

59. Subramanian, A. *et al.* Gene set enrichment analysis: a knowledge-based approach for interpreting genome-wide expression profiles. *Proc Natl Acad Sci U S A* **102**, 15545–15550 (2005).

60. Le Cao, K.A., Boitard, S. & Besse, P. Sparse PLS discriminant analysis: biologically relevant feature selection and graphical displays for multiclass problems. *BMC Bioinformatics* **12**, 253 (2011).

61. Papuchon, J. *et al.* Resistance mutations and CTL epitopes in archived HIV-1 DNA of patients on antiviral treatment: toward a new concept of vaccine. *PLoS One* **8**, e69029 (2013).

62. Ueno, T., Fujiwara, M., Tomiyama, H., Onodera, M. & Takiguchi, M. Reconstitution of anti-HIV effector functions of primary human CD8 T lymphocytes by transfer of HIV-specific αβ TCR genes. *Eur J Immunol* **34**, 3379–3388 (2004).

63. Imataki, O. *et al.* IL-21 can supplement suboptimal Lck-independent MAPK activation in a STAT-3-dependent manner in human $CD8^+$ T cells. *J Immunol* **188**, 1609–1619 (2012).

FIGURES & LEGENDS

FIGURE 1

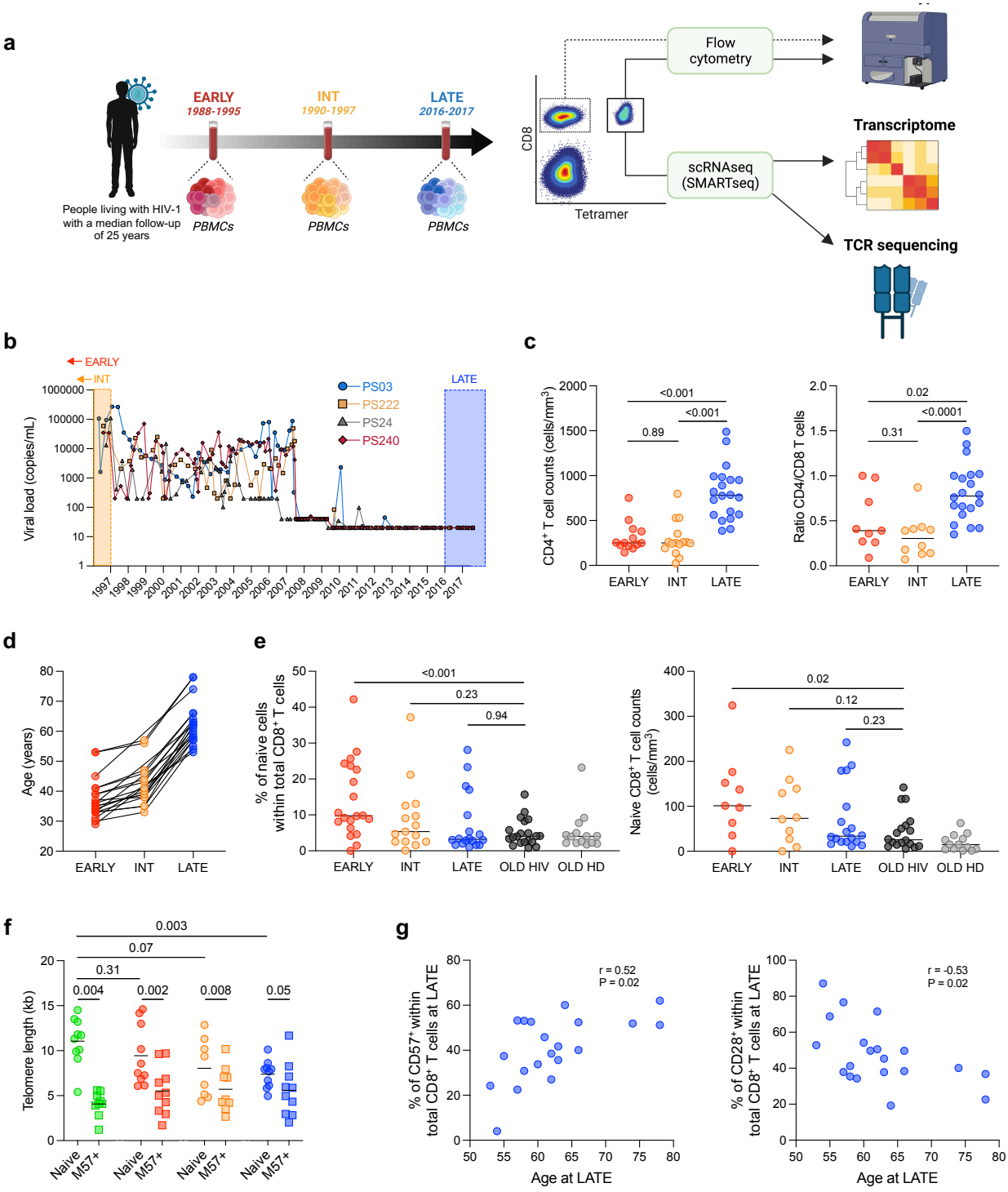

Figure 1 — Ageing and infection history of PLWH.

(**a**) Graphical representation of the experimental approach. (**b**) Viral load trajectories in representative patients (n = 4) from February 1996 to October 2017. EARLY, INT, and LATE time points are highlighted in red, orange, and blue, respectively. (**c**) Absolute CD4$^+$ T cell

counts (EARLY, n = 14; INT, n = 15; LATE, n = 20) and CD4/CD8 ratios (EARLY, n = 9; INT, n = 10; LATE, n = 20). Bars indicate median values. Each dot represents one donor. P values were determined using a two-tailed Mann–Whitney U test. (**d**) Age of individuals from the IMMUNOCO cohort at the EARLY (n = 20), INT (n = 15), and LATE time points (n = 20). (**e**) Left: frequencies of naive $CD8^+$ T cells (EARLY, n = 20; INT, n = 15; LATE, n = 18; OLD HIV, n = 20; OLD HD, n = 14). Right: absolute counts of naive $CD8^+$ T cells (EARLY, n = 9; INT, n = 10; LATE, n = 18; OLD HIV, n = 18; OLD HD, n = 13). Bars indicate median values. Each dot represents one donor. P values were determined using a two-tailed Mann–Whitney U test. HD, healthy donor. (**f**) Telomere lengths in flow-sorted naive and $CD57^+$ memory $CD8^+$ T cell populations from young infected adults (green; age, 25–40 years; n = 10) and individuals from the IMMUNOCO cohort (EARLY, n = 10; INT, n = 9; LATE, n = 10) color-coded as in (**a**). Bars indicate median values. Each dot represents one donor. P values were determined using a two-tailed Mann–Whitney U test. (**g**) Expression of CD28 and CD57 among total $CD8^+$ T cells at the LATE time point plotted as a function of age. Correlations were determined using Spearman's rank test.

FIGURE 2

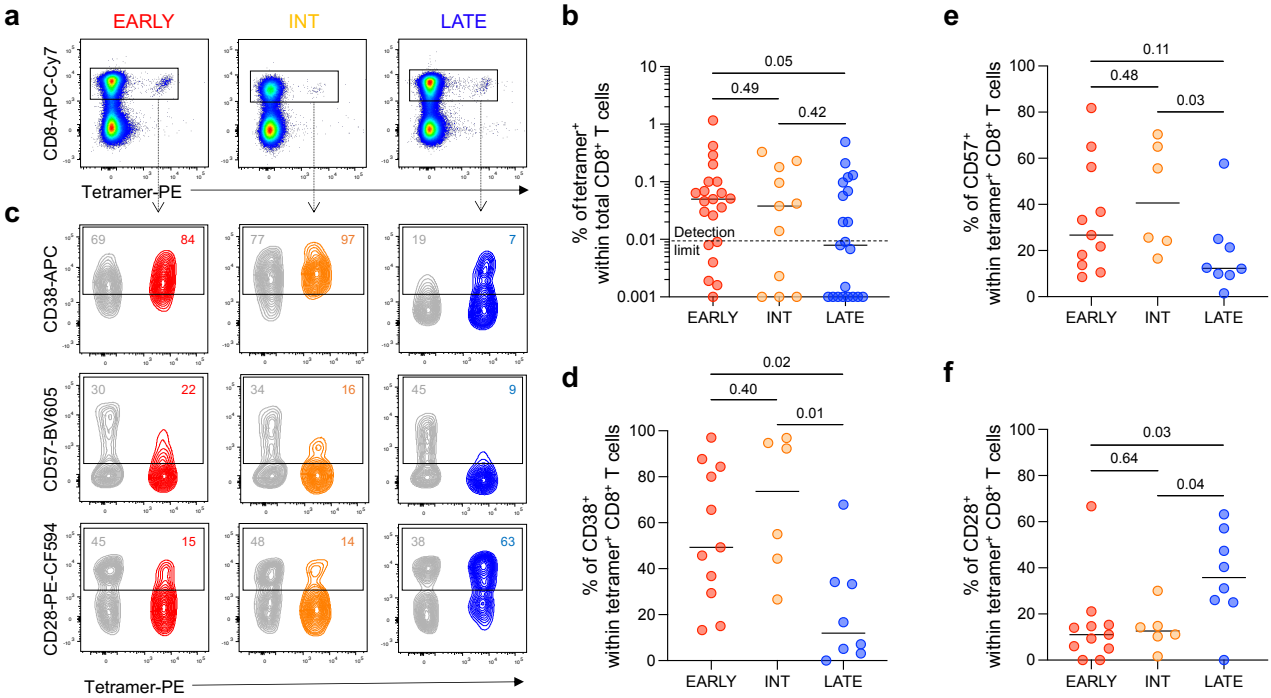

Figure 2 — Phenotypic analysis of HIV-1-specific CD8⁺ T cells.

(**a**) Representative flow cytometry plots showing EI8/HLA-B*08:01 tetramer staining of CD8⁺ T cells at the EARLY, INT, and LATE time points from donor PS24. (**b**) Frequencies of tetramer⁺ CD8⁺ T cells at each time point (EARLY, *n* = 21; INT, *n* = 11; LATE, *n* = 21). Bars indicate median values. Each dot represents a distinct tetramer⁺ population. *P* values were determined using a two-tailed Mann–Whitney U test. (**c**) Representative flow cytometry plots showing the expression of CD28 (top), CD38 (middle), and CD57 among total and EI8-specific CD8⁺ T cells (bottom) identified in (**a**). Numbers indicate percentages in the drawn gates. (**d**–**f**) Frequencies of tetramer⁺ CD8⁺ T cells expressing CD38 (**d**), CD57 (**e**), or CD28 (**f**) at each time point (EARLY, *n* = 11; INT, *n* = 6; LATE, *n* = 8). Bars indicate median values. Each dot represents a distinct tetramer⁺ population. *P* values were determined using a two-tailed Mann–Whitney U test.

FIGURE 3

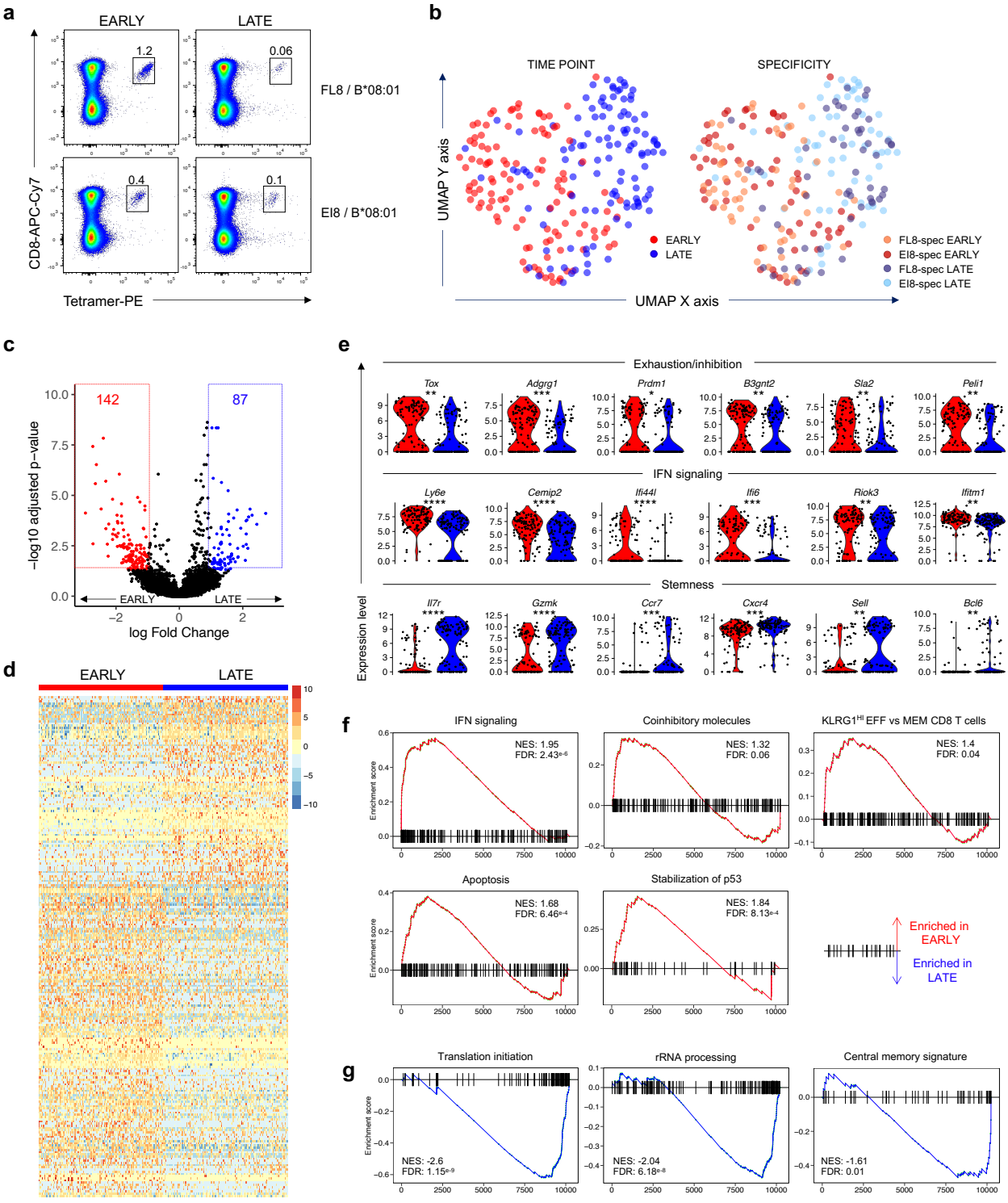

Figure 3 — Transcriptomic analysis of HIV-1-specific CD8$^+$ T cells.

(**a**) Representative flow cytometry plots showing EI8/HLA-B*08:01 and FL8/HLA-B*08:01 tetramer staining of CD8$^+$ T cells at the EARLY and LATE time points from donor PS24. Numbers indicate percentages in the drawn gates. (**b**) UMAP projection of tetramer$^+$ CD8$^+$ T cells. Each dot represents one cell. Each cell was color-coded according to time point (left) or

specificity (right). (**c**) Volcano plot showing differentially expressed genes between the EARLY and LATE time points (red, upregulated at EARLY; blue, upregulated at LATE). The x-axis represents log fold change, and the y-axis represents $-\log_{10}$-adjusted *P* values. (**d**) Heatmap representation of the top 229 differentially expressed genes between the EARLY and LATE time points as defined in (**c**). Significance was determined using a Wilcoxon unpaired test. (**e**) Violin plots showing genes associated with exhaustion and inhibition (top), IFN signaling (middle), and stemness (bottom) at the EARLY (red) and LATE time points (blue). Each violin represents the probability density at each value. Each dot represents one cell. **P* < 0.05, ***P* < 0.01, ****P* < 0.001, *****P* < 0.0001 (FDR-adjusted values). Significance was determined using a Wilcoxon unpaired test. (**f**) GSEA showing the enrichment of genes associated with IFN signaling, coinhibitory molecules, effector differentiation, apoptosis, and stabilization of p53 among EARLY cells. FDR-adjusted *P* values are shown. NES, normalized enrichment score. (**g**) GSEA showing the enrichment of genes associated with protein translation, rRNA processing, and central memory differentiation among LATE cells. FDR-adjusted *P* values are shown. NES, normalized enrichment score.

FIGURE 4

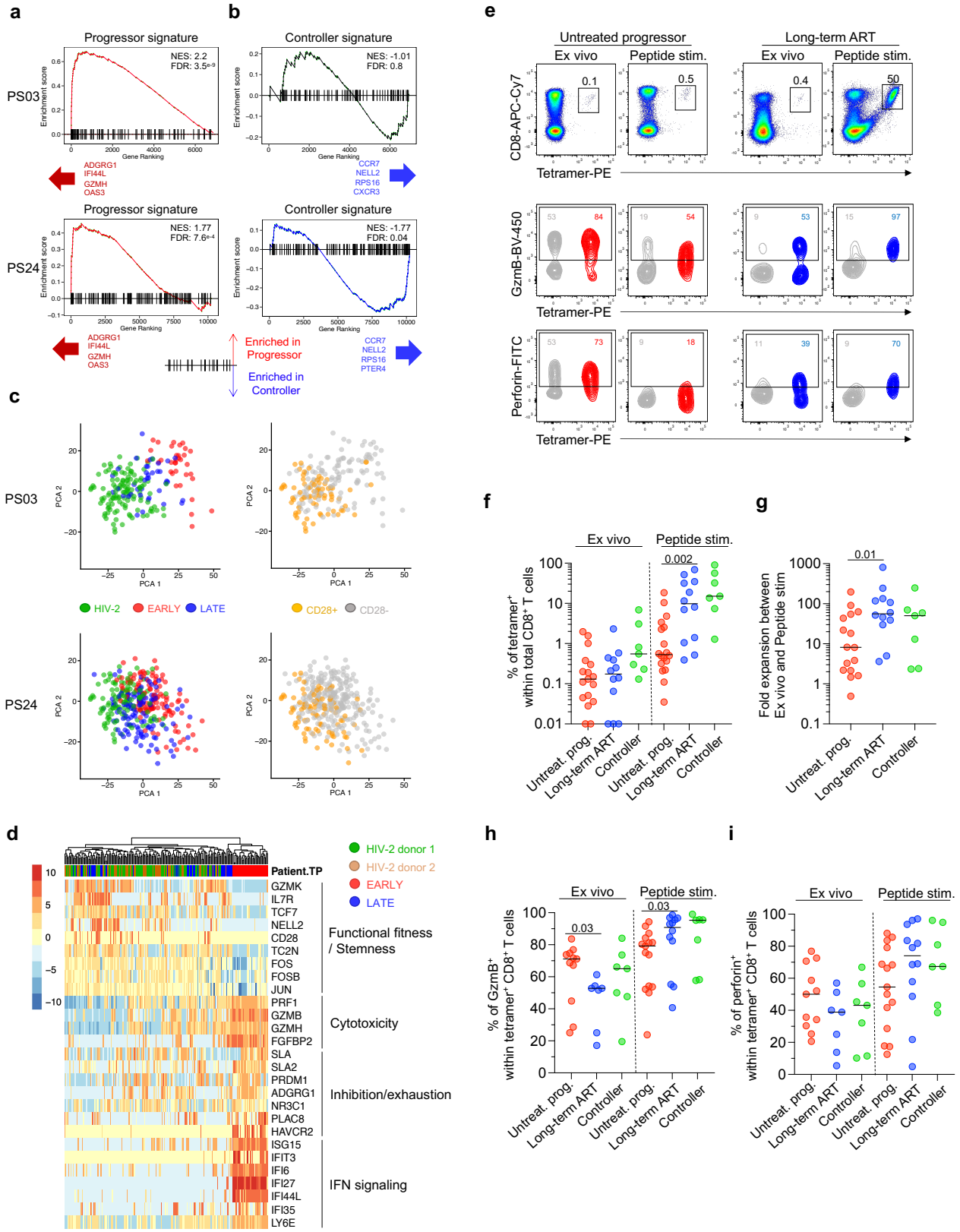

Figure 4 — Gene signatures and functional potential of HIV-1-specific CD8⁺ T cells.

(**a**) GSEA showing the enrichment of genes associated with the progressor phenotype among EARLY cells from donors PS03 and PS24. FDR-adjusted *P* values are shown. NES, normalized

enrichment score. (**b**) GSEA showing the enrichment of genes associated with the controller phenotype among LATE cells from donors PS03 and PS24. FDR-adjusted *P* values are shown. NES, normalized enrichment score. (**c**) PCA plots showing the segregation between EARLY and HIV-2/LATE cells (left) and the corresponding overlap with cells expressing CD28 (right) from PS03. (**d**) Heatmap representation of differentially expressed genes between EARLY and LATE cells from donor PS03 and HIV-2-specific $CD8^+$ T cells (n = 2 donors). (**e**) Representative flow cytometry plots showing tetramer staining of HIV-1-specific $CD8^+$ T cells (top) and the expression of granzyme B (middle) and perforin among total and $tetramer^+$ $CD8^+$ T cells (bottom) before (day 0) and after cognate peptide stimulation of PBMCs (day 12) from an untreated progressor (left) and a donor treated with long-term ART (right). Numbers indicate percentages in the drawn gates. (**f**) Frequencies of $tetramer^+$ $CD8^+$ T cells before (day 0) and after cognate peptide stimulation of PBMCs (day 12) from untreated progressors (n = 17–18), PLWH treated with long-term ART (n = 12), and natural controllers (n = 7). (**g**) Fold change in the frequencies of $tetramer^+$ $CD8^+$ T cell before (day 0) and after cognate peptide stimulation of PBMCs (day 12) from untreated progressors (n = 16), PLWH treated with long-term ART (n = 12), and natural controllers (n = 7). (**h**, **i**) Frequencies of $tetramer^+$ $CD8^+$ T cells expressing granzyme B (**h**) or perforin (**i**) before (day 0) and after cognate peptide stimulation of PBMCs (day 12) from untreated progressors (n = 11–15), PLWH treated with long-term ART (n = 7–12), and natural controllers (n = 7). (**f**–**i**) Bars indicate median values. Each dot represents a distinct $tetramer^+$ population. *P* values were determined using a two-tailed Mann–Whitney U test.

FIGURE 5

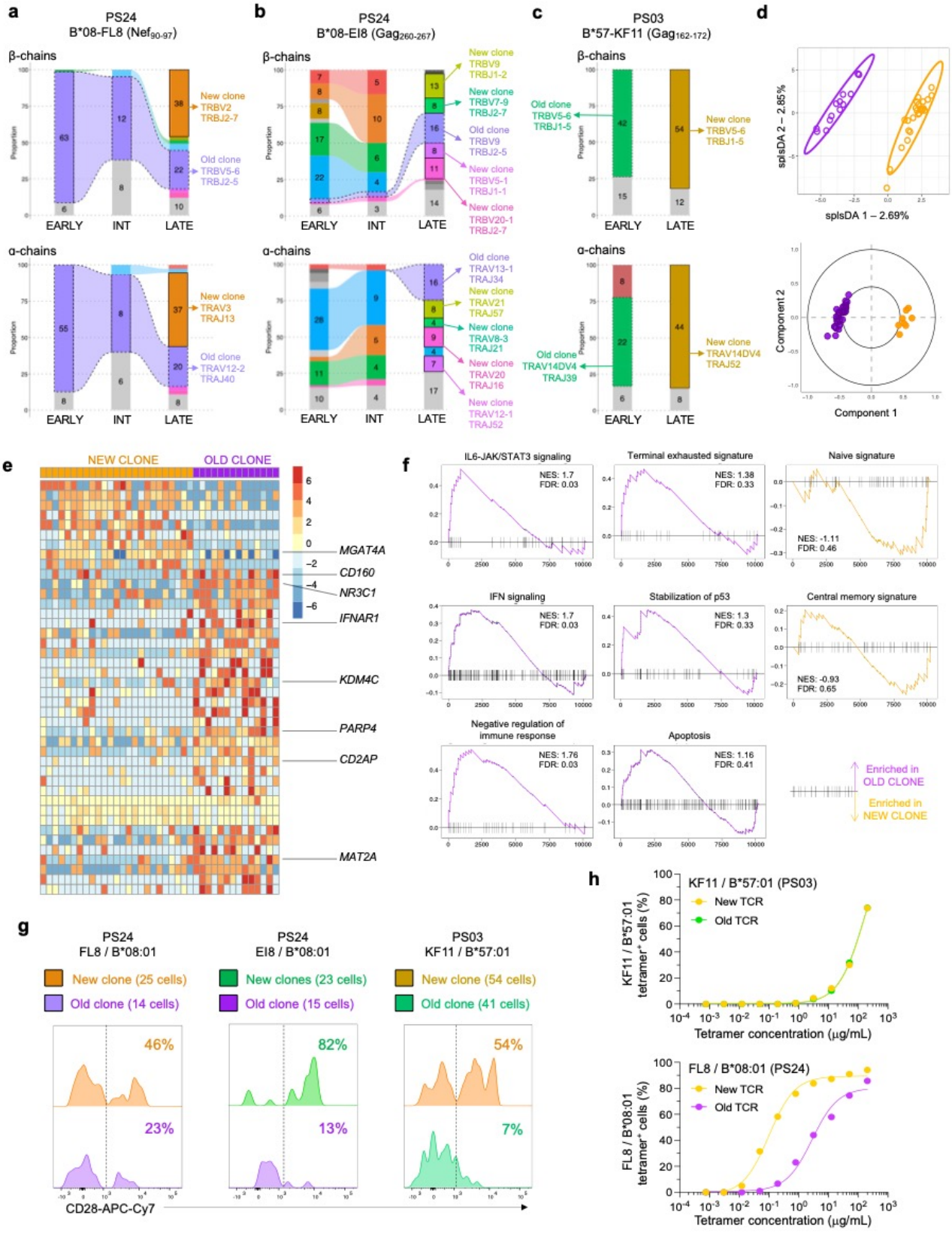

Figure 5 — Clonal evolution of HIV-1-specific CD8⁺ T cells.

(**a**–**c**) Evolution of FL8-specific (**a**) and EI8-specific clonotypes (**b**) from donor PS24 and KF11-specific clonotypes (**c**) from donor PS03. Each color represents a distinct clonotype paired for TCRβ (top) and TCRα (bottom). Solid and dashed lines represent newly detected and old clonotypes, respectively. Alluvial flows are colored to highlight shared clonotypes over time. Sequences identified in only one cell are shown merged in grey. Numbers indicate cells per clonotype. (**d**) Segregation of old (violet) and newly detected FL8-specific clonotypes (orange) from donor PS24 based on gene expression at the LATE time point. Top: sample representation of the two clonotypes using the first two components of the sPLS-DA. Right: projection of sPLS-DA-selected variables on correlation circles. (**e**) Heatmap representation of differentially expressed genes between the two clonotypes as defined in (**d**). Highlighted genes are associated with exhaustion or inhibition. (**f**) GSEA showing the enrichment of genes associated with IL6-JAK/STAT3 signaling, terminal exhaustion, IFN signaling, stabilization of p53, negative regulation of the immune response, and apoptosis in the old clonotype (violet) or naive and central memory differentiation in the newly detected clonotype (orange) as defined in (**d**). (**g**) Index-linked expression of CD28 on old and newly detected clonotypes as defined in (**a**–**c**). (**h**) Tetramer titration curves for Jurkat cells transduced with KF11-specific TCRs from donor PS03 (top) or FL8-specific TCRs from donor PS24 (bottom).

ACKNOWLEDGMENTS

We thank all donors for participating in this study. TCR-deficient Jurkat cells were kindly provided by Takamasa Ueno (Kumamoto University, Japan). We also thank Paul Goepfert (University of Alabama, USA) for assistance with the identification of appropriate donors to confirm the primary findings of this study, David Ambrozak and Noemia Santana Lima for assistance with flow cytometry at Vaccine Research Center (NIAID, NIH, USA), and Vincent Pitard and Atika Zouine for assistance with flow cytometry at the University of Bordeaux (CNRS UMS 3427, INSERM US 005, Bordeaux, France).

FUNDING

This work was funded by INSERM and the University of Bordeaux (Senior IdEx Chair) and by grants from the ANR (14CE16002901), the ANRS (2016-A00400-51), and the Japan Agency for Medical Research and Development (JP22fk0410052). E.W. was supported by Sidaction and Sorbonne University. D.A.P. was supported by a Wellcome Trust Senior Investigator Award (100326/Z/12/Z).

AUTHOR CONTRIBUTIONS

B.A. and V.A. conceived the study; E.W., L.P., K.S., A.R.H., D.C.R., P.R.-P., D.A.P., M.-A.A., D.C.D., and V.A. designed and/or performed experiments; E.W., L.P., A.S., K.S., B.H., D.C.R., S.A.M., S.D., Y.D., Y.S., R.T., C.K., and V.A. analyzed data; A.S., Y.D., S.L.-L., F.B., S.A.M., D.A.P., C.K., and D.C.D. provided reagents, resources, and/or samples; L.C., D.A.P., and V.A. acquired funding; D.A.P., D.C.D., and V.A. supervised the work; E.W., L.P., D.A.P., and V.A. wrote the manuscript. All authors contributed intellectually.

COMPETING INTERESTS

The authors have no conflicts of interest to declare.

DATA AVAILABILITY

All data reported in this paper will be shared by the lead contact upon request.

LIST OF ADDITIONAL MATERIALS

- SUPPLEMENTARY TABLE 1 — Clinical characteristics of participants in this study.
- EXTENDED DATA FIGURE 1 — Viral load and $CD4^+$ T cell trajectories.
- EXTENDED DATA FIGURE 2 — Additional phenotypic analysis of HIV-1-specific $CD8^+$ T cells.
- EXTENDED DATA FIGURE 3 — Transcriptomic analysis of KF11-specific $CD8^+$ T cells from donor PS03.
- EXTENDED DATA FIGURE 4 — Phenotypic and transcriptomic comparisons with HIV-2-specific $CD8^+$ T cells.
- EXTENDED DATA FIGURE 5 — Viral epitope sequences.
- EXTENDED DATA FIGURE 6 — Clonotypic analyses of HIV-1-specific $CD8^+$ T cells.
- EXTENDED DATA FIGURE 7 — Longitudinal analysis of KK10-specific $CD8^+$ T cells from donor VA02.
- EXTENDED DATA FIGURE 8 — TCR transduction of Jurkat cells.
- EXTENDED DATA FIGURE 9 — Flow cytometric gating strategy.